# University of California

# Ernest O. Lawrence Radiation Laboratory

ATOMIC CAPTURE OF $\mu^-$ MESONS IN CHEMICAL COMPOUNDS

TWO-WEEK LOAN COPY

This is a Library Circulating Copy
which may be borrowed for two weeks.
For a personal retention copy, call
Tech. Info. Division, Ext. 5545

## DISCLAIMER

This document was prepared as an account of work sponsored by the United States Government. While this document is believed to contain correct information, neither the United States Government nor any agency thereof, nor the Regents of the University of California, nor any of their employees, makes any warranty, express or implied, or assumes any legal responsibility for the accuracy, completeness, or usefulness of any information, apparatus, product, or process disclosed, or represents that its use would not infringe privately owned rights. Reference herein to any specific commercial product, process, or service by its trade name, trademark, manufacturer, or otherwise, does not necessarily constitute or imply its endorsement, recommendation, or favoring by the United States Government or any agency thereof, or the Regents of the University of California. The views and opinions of authors expressed herein do not necessarily state or reflect those of the United States Government or any agency thereof or the Regents of the University of California.

Submitted to Nuovo Cimento UCRL-10671

UNIVERSITY OF CALIFORNIA

Lawrence Radiation Laboratory
Berkeley, California

Contract No. W-7405-eng-48

# ATOMIC CAPTURE OF $\mu^-$ MESONS IN CHEMICAL COMPOUNDS

Jagdish S. Baijal, Justo A. Diaz, Selig N. Kaplan,
and Robert V. Pyle

March 15, 1963

# ATOMIC CAPTURE OF $\mu^-$ MESONS IN CHEMICAL COMPOUNDS

Jagdish S. Baijal, Justo A. Diaz, Selig N. Kaplan,
and Robert V. Pyle

Lawrence Radiation Laboratory
University of California
Berkeley, California

March 15, 1963

Summary. -Experimental studies of the relative $\mu^-$ meson atomic-capture probabilities in the compounds CuO, $Sb_2O_3$, PbO, CuS, $Sb_2S_3$, PbS, and in the metallic solutions $Ag_{.58}Li$, $CuAu_{.18}$ have been made to test the predictions of the "Fermi-Teller Z-law." In our experiment the capturing atom was identified by decomposing a compound lifetime curve obtained by detecting neutrons from $\mu^-$ capture. The measured atomic-capture ratios are:

| | |
|---|---|
| Cu/O = 6.14 ± 0.35, | Sb/S = 1.64 ± 0.10, |
| Sb/O = 1.86 ± 0.096, | Pb/S = 2.87 ± 0.35, |
| Pb/O = 4.56 ± 0.53, | Ag/Li = 11.66 ± 3.39, |
| Cu/S = 1.89 ± 0.18, | Au/Cu = 0.34 ± 0.032. |

Assuming the Z dependence of the atomic-capture probability can be expressed as proportional to $Z^n$ (n being any positive or negative number), we find that our experimental results fall approximately in the range $n = 1/2$ to $n = 3/2$, where $n = 1$ corresponds to the theoretical prediction of Fermi and Teller.

## I. -Introduction

A theoretical study of the slowing down process of μ mesons in condensed matter was made by Fermi and Teller.[1] They showed that the time required for the muon to slow down, become bound to an atom, and fall into the ground state of the mesonic atom system is small compared to the muon lifetime.

They also estimated the relative atomic-capture rates of mesons by the elements of a chemical compound.[1] They assumed that the probability of capture by a particular atom is just the probability that a slow meson will fall into a negative energy state in the neighborhood of the atom and that this probability is proportional to the rate of energy loss of the meson near zero energy. They calculated that this rate of energy loss is proportional to the atomic number, Z, and therefore concluded that the relative capture probability should be proportional to the atomic-number ratio weighted by atomic concentration. This conclusion is referred to as the "Fermi-Teller Z-law."

The investigation of the relative capture probabilities in atomic mixtures is of itself an interesting topic in atomic physics; moreover, such information is often required in the interpretation of other types of meson interaction experiments where it is desirable or necessary that the target be in a compound form.

Over the past several years a number of experiments have been reported in the literature concerning the relative atomic-capture probabilities of μ-mesons in chemical compounds.[2-7]

The first experiment specifically designed to test the "Z-law" was carried out by Stearns and Stearns, who compared the relative yields of mesic x-rays in CaS and $Al_2O_3$, using compounds and macroscopic mixtures of the same composition.[2] They assumed that the stopping power per atom is proportional to the atomic number and were then able to deduce that the atomic capture of mesons in CaS and $Al_2O_3$ was also proportional to Z.

Sens et al. questioned the conclusions of Stearns and Stearns on the basis that the atomic stopping power, which had been assumed proportional to Z, is in fact not accurately known at low meson energies.[3] Sens et al. experimentally investigated the meson capture in several compounds by detecting the decay electrons from mesons bound in atomic orbits. Knowing the mean lifetime of μ-mesons in each element, and the branching ratio between decay and capture, they were able to unfold the curves and obtain the relative atomic-capture probabilities. They reported that their results are more nearly independent of the atomic number than proportional to Z.

More recently several other groups of experimenters have reported measurements obtained through techniques similar to those of Sens et al. (i.e., through the detection of electrons from the decay of bound muons). On the basis of these results, which are summarized in Table I, it seems safe to say that no general rule regarding the capture dependence on the atomic number can be deduced from the experimental evidence to date.

We have investigated this phenomenon using a different technique, namely, the detection of neutrons from μ-interactions with nuclei. As in previous experiments the approach is to decompose a composite lifetime curve obtained from a compound into two constituents, each of which corresponds to

a particular element. The intercepts at zero time for each curve can then be used to find the relative numbers of μ-mesons arriving at the mesic K shells of different atomic species. For those targets in which the neutron yield from the lighter element is very small the capture rate is obtained by comparing neutron yields from the compound target with an elemental target of the heavier constituent. In heavier elements ($Z > 10$), where it is more probable that a μ meson will be captured by the nucleus than it will decay into an electron, we believe that there are fewer corrections associated with the detection of neutrons from nuclear capture than from the detection of decay electrons. It can also be shown that it is better to limit the detection to neutrons because of additional background problems associated with nuclear γ rays.[8]

The choice of target materials was governed both by the demands of the experimental technique and by the hope of maximizing the likelihood of observing any clear-cut systematics in capture ratios in the available experimental time. The prime requirement was that there be great enough difference in atomic number of the constituent elements so that nuclear-capture rates could be clearly distinguished and so that the sensitivity of the results to any Z dependence would be maximized.

In the hope of reducing confusion resulting from effects of different kinds of chemical binding, we chose as targets the oxides and sulfides of three metals with widely different atomic numbers. Although the particular choice of the metals was arbitrary, the sulfur and oxygen were chosen because they both belonged to the same periodic group (Group VI), their compounds were readily available, and because of the rather remarkable results previously observed in oxides by Sens et al.[2] Unfortunately, the present technique did not conveniently

lend itself to a repetition of any of the measurements on the lighter compounds measured by Sens.

Two metallic solutions, AgLi and CuAu, were also chosen because of their homogeneous structure[9]--and because electrically conducting compounds should most closely approximate the conditions of the Fermi-Teller theory.

## 2. -Experimental arrangement.

The Magnet system and the beam.--Negative pions were produced by bombarding a 2-in.-thick Be target in the 184-inch cyclotron with 730 MeV protons. Some of these pions immediately decayed into muons near the target. These pions and muons were momentum-analyzed by the fringing field and passed out of the cyclotron vacuum tank through a thin aluminum window. The beam then entered the meson cave through an 8-ft.-long iron collimator. Further momentum analysis was provided by a 50-deg bend through an H magnet. The beam then passed through a 4 × 4-in. aperture in a Pb collimator into a low-background room made from 4-ft.-thick concrete blocks.

The beam was monitored by a coincidence telescope consisting of two 4×4×1/4-in. plastic scintillators, $S_1$ and $S_2$, placed as shown in Fig. 1. The signal from another coincidence, anticoincidence, telescope, $S_3S_4\overline{AC}$, signified the stopping of a meson in the target. The plastic scintillators $S_3$ and $S_4$ were the same size as $S_1$ and $S_2$. The water Cerenkov counter C was 5×5×2 in., and served to veto coincidence pulses produced by electrons in the beam. The 7-in. diam scintillation counter A, vetoed particles that passed through the target without stopping.

Two things were done to minimize the neutron background caused by stopping pions. First, $CH_2$ was used as the absorbing material to minimize neutron production from $\pi^-$ stoppings and to act as a moderator for neutrons produced along the beam path. Second, an effort was made to maximize the $\mu/\pi$ ratio with a minimum loss of $\mu$ intensity.

The latter was accomplished by first varying the position of the internal Be target to optimize the total flux through the telescope. Then the bending-magnet current was increased about 10%. While reducing somewhat the $\mu$ intensity it also increases the $\mu/\pi$ ratio from 1/5 to somewhat better than 3/1. This is because the $\pi$ source was essentially the size of the target, whereas muons being produced in $\pi$ decay, had a more diffuse source. By detuning the magnet we shifted the apparent-source position away from the center of the target, thus reducing both the $\pi$ and $\mu$ intensities, but the effect on the $\pi$'s was much greater than on the $\mu$'s.[10]

In Fig. 2 we show a differential range curve taken after we detuned the magnet. The $\pi^-$ peak is at 8.5 in. of $CH_2$ and the $\mu^-$ peak at 12.5 in. The stopping rate in a 5 g/cm$^2$ target over the area defined by the 4×4-in. counter was about 17,000/min.

Electronics.—A schematic diagram of the electronics is shown in Fig. 1. The signal, $S_3S_4\overline{AC}$, indicating a $\mu^-$ stop in the target, triggered a gate generator, G, which produced a "gate pulse" 3 μsec wide. This pulse and a signal $N\overline{A}$ (designating uncharged particles that interacted in N) were fed into a coincidence circuit (K) whose output provided a "start" pulse for the time-to-height converter (THC). The signal, $N\overline{A}$ was delayed about 1.25 μsec, as shown in Fig. 3. The $N\overline{A}$ pulses that appeared within the first 1.25 μsec were therefore uncorrelated with muons and hence gave a measurement of the background.

The "stop" pulse for the THC came from the output of the coincidence, $S_3S_4\overline{AC}$, delayed by about 2.5 μsec. The delay was introduced because the THC was stopped by the $\mu^-$ stop signal, which appeared earlier than the "start" signal. Since the coincidence output of K (start signal) anticipated the presence of a stop signal, the THC worked only when there was a useful event, thereby minimizing dead time. The THC produced a pulse whose height was proportional to a constant minus the time delay between radiation emission and muon stopping in the target. This pulse was analyzed in a Nuclear-Data 101 pulse-height analyzer (PHA) which was gated with a signal generated by a pulse-shape discriminator which differentiates between neutron and gamma pulses in the N counter. This discriminator is described in more detail below.

The time-to-height converter was an Eldorado Model TH 300[11] modified to eliminate the rising ramp of the THC output so that all the pulses had the same rise time (Fig. 3).

The linearity of the THC and PHA system was checked by simulating the coincidence, $N\overline{A}$ with a pulser having a repetition rate of 10 kc/sec. The output of the $\mu^-$ stop signal, $S_3S_4\overline{AC}$, was simulated by the $S_3$ scintillation counter alone counting a $Na^{24}$ source. The radioactive source provided stop pulses which occurred randomly in time. Because the time intervals between the occurrence of a start pulse and the following stop pulse were of random lengths, the spectrum displayed on the PHA was a random-height spectrum and, for linear behavior of both the THC and PHA, should give equal probability of a pulse appearing in each channel. The data from a typical run are shown in Fig. 4. These data were fitted to a lifetime curve of the form $N = N_0 e^{-\lambda t}$ where t was the channel number and λ was allowed to take on both

positive and negative values. Varying both $N_0$ and $\lambda$ gave a best fit with $\lambda = (2.2 \pm 4.6) \times 10^{-5}$/ch$^{-1}$ indicating a high degree of linearity over the channel range. Some nonlinearity was observed at both the high and low ranges of the analyzer but neither of these regions were used in the analysis.

We calibrated the THC and accurately located zero time by using the incident meson beam and removing the polyethylene absorber, taking $\overline{A}$ and the pulse shape discrimination from the circuit and reducing the beam intensity. The delay, D was then varied using length RG-63U cable with precisely measured transmission times. Six delay times over the analyzer range were measured. The counts for a particular delay had a distribution with a full width of less than two channels. The centroid was found by weighting each channel in proportion to the number of counts in it. The time calibration data were fitted to a straight line to obtain an average time/channel (which was about 9.0 nsec). All measured points agreed with this line to within 0.2 channels. This calibration was performed at frequent intervals throughout the course of the experiment.

Neutron counter and pulse-shape discriminator.—To detect neutrons in the presence of $\gamma$ rays, we used a pulse-shape discriminator with the neutron scintillation counter. This discriminator was essential, since in its absence the rate of detection of $\gamma$ rays was comparable with that of neutrons.

The neutron counter consisted of a 5-in. -diam × 1-in. thick liquid scintillator, NE 212,[12] contained in a thin-walled glass cylinder. This glass container was attached to an RCA 7046 photomultiplier tube through a lucite light pipe. The scintillator was flushed continuously with dry argon gas to remove oxygen, since oxygen in liquid scintillators destroys the pulse-shape discrimination properties.

This discrimination circuit differs in detail in two respects from most of those reported in the literature [13] First, the two pulses that sample the shape of the scintillator light pulses were generated at the same electrode of the phototube (dynode 14) so that fast signals could be extracted from the anode without any mutual interference. Second, the two shape-information pulses were extracted separately from the phototube and the actual comparison and discrimination was accomplished in a counting area that was about 200-ft removed from the detector. This permitted remote monitoring of the counter operation. The basic circuit, as pictured in Fig. 5, is an adaptation of a circuit suggested by Dr. Robert Mather.[14]

3.-Experimental procedure and data reduction.

The time distribution of neutrons following capture in each of the elemental and compound targets was measured. To find the relative atomic-capture probability, we compared the relative captures in the constituents of the compound with those in the separate elements. The compound and the separate elements were run consecutively to minimize the effects of possible long-term time drifts. The energy threshold of the PSD was set to give neutron acceptance with long-term stability and essentially 100% $\gamma$ rejection. Some 3000 neutrons above an energy of about 2 MeV were collected in an hour for $10^6$ $\mu^-$-meson stoppings in a target of 5 g/cm$^2$. Each target was run at least twice.

The constancy of the neutron counter sensitivity was checked at regular intervals with a PuBe source in a fixed geometry; during the course of the run the counting rate did not vary by more than 1%.

The data recorded during the various runs were the number of $\mu^-$-meson stoppings and the time distribution of neutrons emitted after the stoppings. The rate of disappearance of $\mu^-$ mesons from the mesic atoms's K orbit can be written as

(1) $$\frac{dN}{dt} = -\Lambda N ,$$

or

(2) $$N = N_0(Z)e^{-\Lambda t} , \quad \text{and} \quad \Lambda = \Lambda_d + \Lambda_c ,$$

where $N_0(Z)$ is the number of muons bound to the K orbit of an element of atomic number Z at t = 0 (this is the same as the total number of mesons stopping), $\Lambda$ is the total disappearance rate and $\Lambda_d$ and $\Lambda_c$ are the muon-decay and nuclear-capture rates, respectively. For a single element the observed neutron time distribution Y(t) can be written as

(3) $$Y(t) = E N_0 \Lambda_c e^{-\Lambda t} + B ,$$

where B is the background rate, and E is the neutron detection efficiency. Similarly, for a binary compound, we have

(4) $$Y(t) = E_1 C_1 N_0 \Lambda_{c1} e^{-\Lambda_1 t} + E_2 C_2 N_0 \Lambda_{c2} e^{-\Lambda_2 t} + B ,$$

where $E_1$ and $E_2$ are the respective neutron detection efficiencies for the constituent elements, and $C_1$ and $C_2$ are the respective atomic-capture probabilities that we want to determine; their sum should be unity.

The neutron time-distribution data were least-squares-fitted to Eqs. (3) and (4) with an IBM 704 program, FRENIC.[15] For an elemental target the measured background and lifetime[15] were held constant and the program calculated the intercept giving the best fit. In the analysis of the compound targets we then inserted the measured background and the measured values of the lifetimes and the program calculated the intercepts at time zero.

In terms of the symbols of Eqs. (3) and (4) the calculated intercepts were $E_1 N_0 \Lambda_{c1}$, $E_2 N_0 \Lambda_{c2}$, $E_1 C_1 N_0 \Lambda_{c1}$, and $E_2 C_2 N_0 \Lambda_{c2}$. The E's of Eq. (3), however, were slightly different from those of Eq. (4) because of geometrical and neutron attenuation differences in the targets. Corrections were made for these effects before calculating $C_1$ and $C_2$.

The details of these corrections, including the separate experimental measurements and calculations are described elsewhere.[16] In all cases the changes in the $C_1/C_2$ ratio produced by these corrections were smaller than the stated statistical errors.

The data from the compounds that contained oxygen or lithium could not be analyzed in quite the same manner because the small nuclear capture rates in the light elements resulted in statistically insignificant neutron yields. In these cases we obtained the relative capture probabilities, $C_1/C_2$, from the subsidiary condition, $C_1 + C_2 = 1$.

Examples of experimental time distributions for single runs are shown in Fig. 6 (It was not convenient to combine graphically all of the runs of a target because of slight variations in time/channel calibration over the course of the experiment.)

## 4. -Results.

The experimental results are given in Table II. The subscripts 1 and 2 designate the higher- and lower-Z components respectively. The ratio $C_1/C_2$ represents the relative atomic capture probability. The sum of the capture probabilities, $C_1 + C_2$ should equal unity and gives, therefore, a check on the measurements. The especially low value of this sum for CuS caused great

concern and led ultimately to a complete chemical analysis of all target materials, which were supposedly reagent grade. The results of this analysis showed that, whereas all other targets were at least 99.8% pure, the CuS and PbS were both contaminated with sulfates. By atomic concentration their chemical compositions were:

$$\text{"CuS"} \rightarrow 0.845\ CuS + 0.155\ (CuSO_4 \cdot 5H_2O)\ ,$$

and

$$\text{"PbS"} \rightarrow 0.934\ PbS + 0.066\ PbSO_4\ .$$

Assuming the number of mesons captured by the oxygen is proportional to its atomic concentration and that the proportionality constants, which are presumably Z dependent, are simply determined from the CuO and PbO results (Table II), we can estimate the fraction of atomic captures by oxygen. We find the values to be $0.12 \pm 0.02$ and $0.038 \pm 0.005$ for the "CuS" and "PbS" respectively. In both cases the values are only half of what is required to make the atomic-capture probabilities add up to unity. We note that the observations of Sens et al.[2] indicate enhanced capture by oxygen in compounds of light elements with oxygen. This effect, operating in the sulfates of our targets could account for the remaining captures. It may also alter the $C_1/C_2$ ratio from that of a pure sulfide but further considerations suggest that the change is rather small. For example, in the case of CuS we can assume that the Cu and S in the sulfate and sulfide capture muons in proportion to the respective molecular concentrations in which case the measured value of $C_1/C_2$ is a weighted average of the capture ratios for the two compounds. For the observed contamination the $C_1/C_2$ ratio for the sulfate can vary between 1.0 and 3.0 (n between 0 and 2 in Eq. 5) and not change the $C_1/C_2$ ratio for CuS by as much as the stated statistical error.

Therefore, despite the unfortunate occurrence of the sulfate contamination, we believe that little, if any, error is produced in the $C_1/C_2$ ratio.

## 5. -Discussion.

To aid in the discussion of the results, let us assume that the ratio of atomic-capture probabilities in a binary compound can be described by a relation of the form

$$C_1/C_2 = a_1/a_2(Z_1/Z_2)^n \quad , \tag{5}$$

where $a_1$ and $a_2$ are the atomic concentrations of the two components and $n$ is any real number. The Fermi-Teller prediction is obtained by setting $n = 1$, whereas capture in proportion to the atomic concentration alone is given by $n = 0$. The results of this experiment (Table II) are summarized in Table III together with the ratios corresponding to $n = 1$ and $n = 0$. The values of $n$ calculated from the experimental results are given in the last column and cover the range $n = 1/2$ to $n = 3/2$. (A similar compilation of previously published measurements is given in Table I.)

The data of Tables I and III are presented graphically in Fig. 7. Although most of the measurements fall in the region of positive $n$ values, there is obviously no simple $Z^n$ dependence, valid for all compounds. One can search for an indication that some class of compounds (for example, alloys or oxides) may separately show a systematic dependence on the atomic number, but the experimental evidence to date is too sketchy to permit definite conclusions.

It seems desirable that the reliability of the data to date should be established before capture in other compounds is investigated (e.g., note the discrepancy between the two LII measurements). Possible systematic effects

resulting from chemical binding can then be examined by investigating, say, oxides of different elements and different lattice structures of the same compound.[18]

The theoretical situation is probably no better than the experimental state. In deriving the Z-law Fermi and Teller neglected details which had been discussed in an earlier part of their paper, e.g. the Brillouin gap in insulators, and were "led by crude estimates to the conclusion that the capture probability is proportional to the nuclear charge Z."[19] Apparently, more reliance has been placed on the result of this calculation than the authors had intended,[20] and considerably more work is required before it will, in fact, be possible to make meaningful comparisons between theory and experiment.

## 6. Acknowledgments.

We wish to express our appreciation to Professor Burton J. Moyer for his support of and continued interest in this work. One of us (R. V. P.) gratefully acknowledges the support of Dr. C. M. Van Atta, which enabled him to participate in this experiment.

We would also like to express our thanks to Dr. Robert L. Mather for his suggestions concerning the pulse-shape discriminator, to Mr. Cordon R. Kerns for the precision calibrations of the delay cables, and to Mr. Gabriel H. Kojoian for his contributions during the planning and execution of the experiment.

This work was done under the auspices of the U. S. Atomic Energy Commission.

7. -Footnotes and references.

(1) E. Fermi and E. Teller, Phys. Rev., 72, 399 (1947).

(2) M. B. Stearns and M. Stearns, Phys. Rev., 105, 1573 (1957).

(3) J. C. Sens, R. A. Swanson, V. L. Telegdi, and D. D. Yovanovitch, Nuovo Cimento, 7, 536 (1958).

(4) J. F. Lathrop, R. A. Lundy, R. A. Swanson, V. L. Telegdi, and D. D. Yovanovitch, Nuovo Cimento, 15, 831 (1960).

(5) A. Astbury, P. M. Hatersley, M. Hussain, M. A. R. Kemp, and H. Muirhead, Nuovo Cimento, 18, 1267 (1960).

(6) G. Backenstoss, B. Block, B. Chidley, R. Reiter, T. Romanowski, R. Siegel, and R. Sutton, Bull. Am. Phys. Soc. II, 4, 273 (1959).

(7) M. Eckhause, T. A. Fillipas, R. B. Sutton, R. E. Welsh, and T. A. Romanowski, Nuovo Cimento, 24, 666 (1962).

(8) J. S Baijal, J. A. Diaz, S. N Kaplan and R. V. Pyle, $\mu^-$ Lifetimes in Medium- and High-Z Elements (to be published).

(9) Max Hansen, The Constitution of Binary Alloys, (McGraw-Hill Book Publishing Co., Inc., New York 1958).

(10) We believe this particular technique was first suggested in a paper by N. Campbell and R. A. Swanson, University of Chicago, 1958 (unpublished).

(11) Manufactured by Eldorado Electronics Company, Berkeley, California.

(12) Manufactured by Nuclear Enterprises, Ltd., Winnipeg, Canada. (Since the performance of this experiment NE 212 has been superceded by (NE213.)

(13) See for example, F. D. Brooks, Nucl. Instr. and Methods, 4, 151-163 (1959).

(14) Robert Mather, U. S. Naval Radiological Defense Laboratory, San Francisco 1959, (private communication).

(15) FRENIC is the program code name for the calculation described by Keepin, Winelt, and Zeigler, J. Nucl. Energy 6, 1 (1957).

(16) J. S. Baijal (Ph. D. Thesis), University of California Lawrence Radiation Laboratory Report UCRL-10429, 1962 (unpublished).

(17) It should be pointed out that the relatively greater meson stopping power of the sulfate resulting from the presence of O and H may augment the captures by Cu and S in the sulfate relative to the sulfide. However, it seems even more likely to us that an enhanced oxygen capture probability would, in fact, diminish the Cu and S captures.

(18) As an example, the lattice structure of the CuAu alloy can be changed from disordered face-centered cubic (present experiment) to ordered face-centered cubic to tetragonal by progressively increasing the percentage of gold. Charles S. Barrett, Structure of Metals, (McGraw-Hill Book Publishing Co., Inc., New York, 1952) Ch. XII, p. 269.

(19) It seems to us that the method outlined in Ref. 1 might lead to a capture probability that is proportional to $Z^{2/3}$ rather than Z.

(20) E. Teller, Lawrence Radiation Laboratory, Berkeley, California (private communication).

8. -Captions.

Fig. 1. Counter arrangement and block diagram of electronics.

Fig. 2. Differential range curve.

Fig. 3. Time relationships of pulses in the electronic circuitry.

Fig. 4. Typical THC and PHA linearity calibration.

Fig. 5. Circuit diagram of phototube base showing pulse shape discriminator. The discriminator is in the dynode 14 circuit as indicated.

Fig. 6. Typical lifetime curves. For display convenience the channel number labeling has been arbitrarily inverted and translated from the actual values as shown in Fig. 4. The time/channel is approximately 9.0 nsec.

Table I. - Summary of "Z law" results from previous workers. Relative numbers of $\mu^-$ mesons reaching the 1S level in the constituents of a compound.

| Compound | Ratio | Observed | Predicted, Fermi and Teller | Atomic ratio | n† |
|---|---|---|---|---|---|
| Sens et al. (Chicago) | | | | | |
| $P_2O_5$ | P/O | 0.371±0.041 | 0.75 | 0.4 | -0.12±0.18 |
| $Al_2O_3$ | Al/O | 0.435±0.038 | 1.084 | 0.66 | -0.88±0.18 |
| $SiO_2$ | Si/O | 0.386± 0.025 | 0.875 | 0.5 | -0.46±0.12 |
| KOH | K/O | 0.455±0.083 | 2.38 | 1.0 | -0.91±0.21 |
| $KHF_2$ | K/F | 0.588±0.138 | 1.053 | 0.5 | 0.19±0.27 |
| $C_6H_4Cl_2$ (Liquid) | Cl/C | 0.435±0.0378 | 0.943 | 0.33 | 0.27±0.083 |
| $C_6H_4Cl_2$ (Solid) | Cl/C | 0.476±0.045 | 0.943 | 0.33 | 0.35±0.091 |
| $CCl_4$ | Cl/C | 4.1±0.8 | 11.3 | 4.0 | 0.024±0.19 |
| Lathrop et al. (Chicago) | | | | | |
| LiI | I/Li | 15.8±2.0 | 17.67 | 1 | 0.96±0.044 |
| AgZn | Ag/Zn | 2.2±0.7 | 1.57 | 1 | 1.75±0.71 |
| Astbury et al. (Liverpool) | | | | | |
| $PbF_2$ | Pb/F | 4.8±0.7 | 4.5 | 0.5 | 1.02±0.07 |
| Backenstoss et al. (Carnegie Tech.) | | | | | |
| AgCl | Ag/Cl | 0.8±0.2 | 2.8 | 1 | -0.22±0.24 |
| LiI | I/Li | 1.3±0.5 | 17.67 | 1 | 0.091±0.13 |
| $UF_4$ | U/F | 0.7±0.3 | 2.6 | 0.25 | 0.44±0.18 |
| Eckhause et al. (Carnegie Tech.) | | | | | |
| $BiF_3$ | Bi/F | 1.58±0.15 | 3.07 | 0.33 | 0.70±0.043 |
| $UF_4$ | U/F | 1.52±0.15 | 2.56 | 0.25 | 0.78±0.043 |
| $CuAl_2$ | Cu/Al | 1.75±0.18 | 1.11 | 0.5 | 1.56±0.13 |

† Assuming that the atomic capture probability goes as $Z^n$ (n being any positive or negative number).

Table II. -Results for atomic-capture probability in the constituents of the compounds.

| Compound | $C_1$ | $C_2$ | $C_1/C_2$ | $C_1+C_2$ |
|---|---|---|---|---|
| CuAu | 0.26 ± 0.023 | 0.77 ± 0.023 | 0.34 ± 0.032 | 1.03 ± 0.032 |
| AgLi | 0.921 ± 0.023 | 0.079 ± 0.023 | 11.66 ± 3.39 | - |
| CuS | 0.51 ± 0.015 | 0.27 ± 0.024 | 1.89 ± 0.18 | 0.78 ± 0.028† |
| $Sb_2S_3$ | 0.59 ± 0.015 | 0.36 ± 0.020 | 1.64 ± 0.10 | 0.95 ± 0.026 |
| PbS | 0.66 ± 0.019 | 0.23 ± 0.027 | 2.87 ± 0.35 | 0.89 ± 0.033† |
| CuO | 0.86 ± 0.019 | 0.14 ± 0.019 | 6.14 ± 0.85 | - |
| $Sb_2O_3$ | 0.65 ± 0.012 | 0.35 ± 0.012 | 1.86 ± 0.096 | - |
| PbO | 0.82 ± 0.020 | 0.18 ± 0.020 | 4.56 ± 0.53 | - |

† These low values were found to be due to contaminated targets. See text.

Table III. -Summary of results. Relative number of $\mu^-$ mesons reaching the mesic K shell in the constituents of a chemical compound.

| Compound | Ratio | Observed | Predicted, Fermi and Teller | Atomic ratio | n |
|---|---|---|---|---|---|
| CuAu† | Au/Cu | 0.34 ± 0.032 | 0.495 | 0.182 | 0.62 ± 0.094 |
| AgLi† | Ag/Li | 11.66 ± 3.39 | 9.1 | 0.58 | 1.08 ± 0.11 |
| CuS | Cu/S | 1.89 ± 0.18 | 1.81 | 1 | 1.07 ± 0.16 |
| $Sb_2S_3$ | Sb/S | 1.64 ± 0.10 | 2.13 | 0.67 | 0.78 ± 0.053 |
| PbS | Pb/S | 2.87 ± 0.35 | 5.12 | 1 | 0.65 ± 0.076 |
| CuO | Cu/O | 6.14 ± 0.85 | 3.62 | 1 | 1.41 ± 0.11 |
| $Sb_2O_3$ | Sb/O | 1.86 ± 0.096 | 4.25 | 0.67 | 0.55 ± 0.028 |
| PbO | Pb/O | 4.56 ± 0.53 | 10.25 | 1 | 0.65 ± 0.050 |

† AgLi and CuAu are metallic solutions. AgLi has 10% of Li by weight. CuAu has 36% of Au by weight.

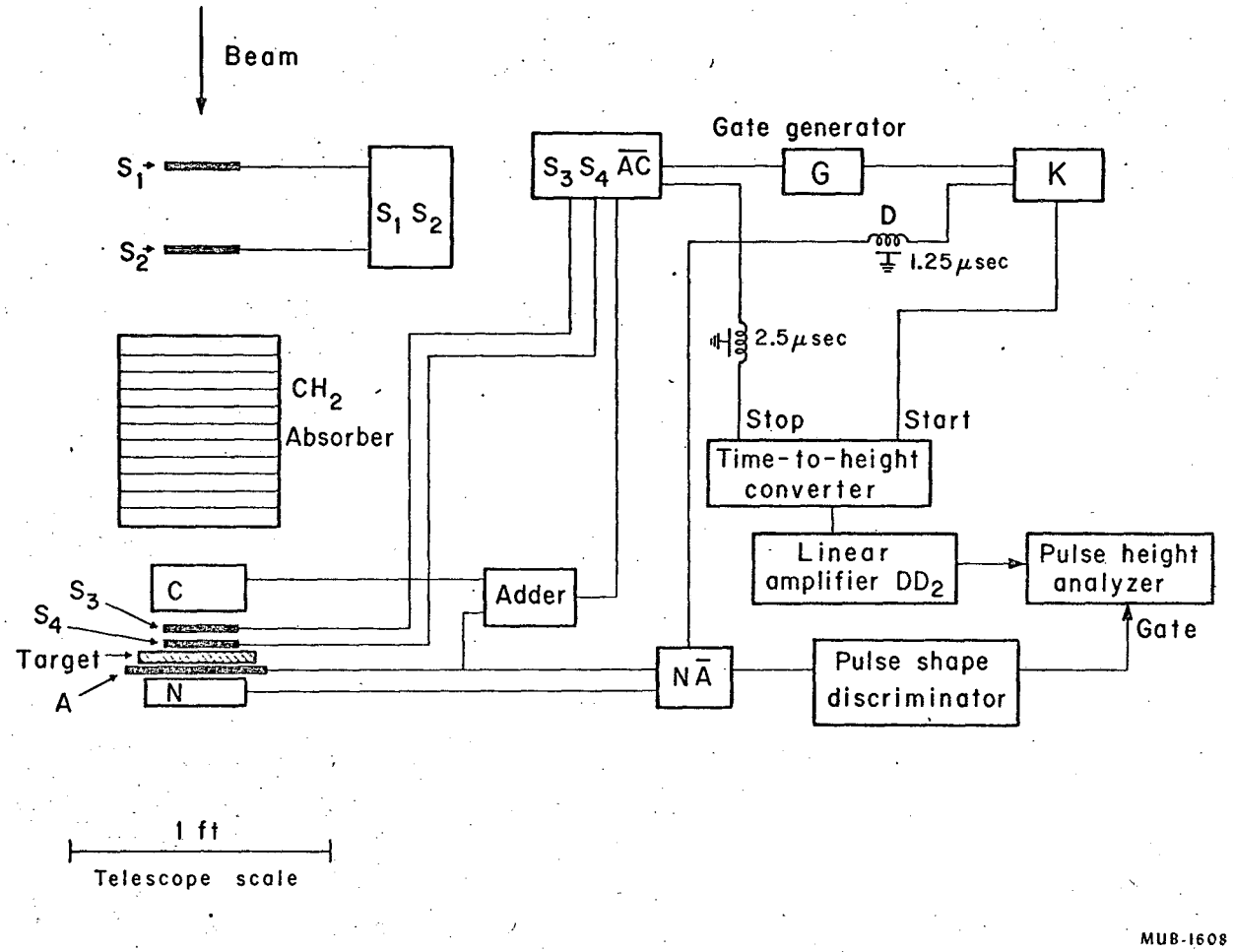
Beam
$S_1$
$S_2$
$S_1$ $S_2$
$S_3$ $S_4$ $\overline{AC}$
Gate generator
G
K
D
1.25 μsec
2.5 μsec
$CH_2$
Absorber
Stop
Start
Time-to-height converter
Linear amplifier $DD_2$
Pulse height analyzer
Gate
C
Adder
$S_3$
$S_4$
Target
A
N
$N\overline{A}$
Pulse shape discriminator
1 ft
Telescope scale
MUB-1608

Fig. 1

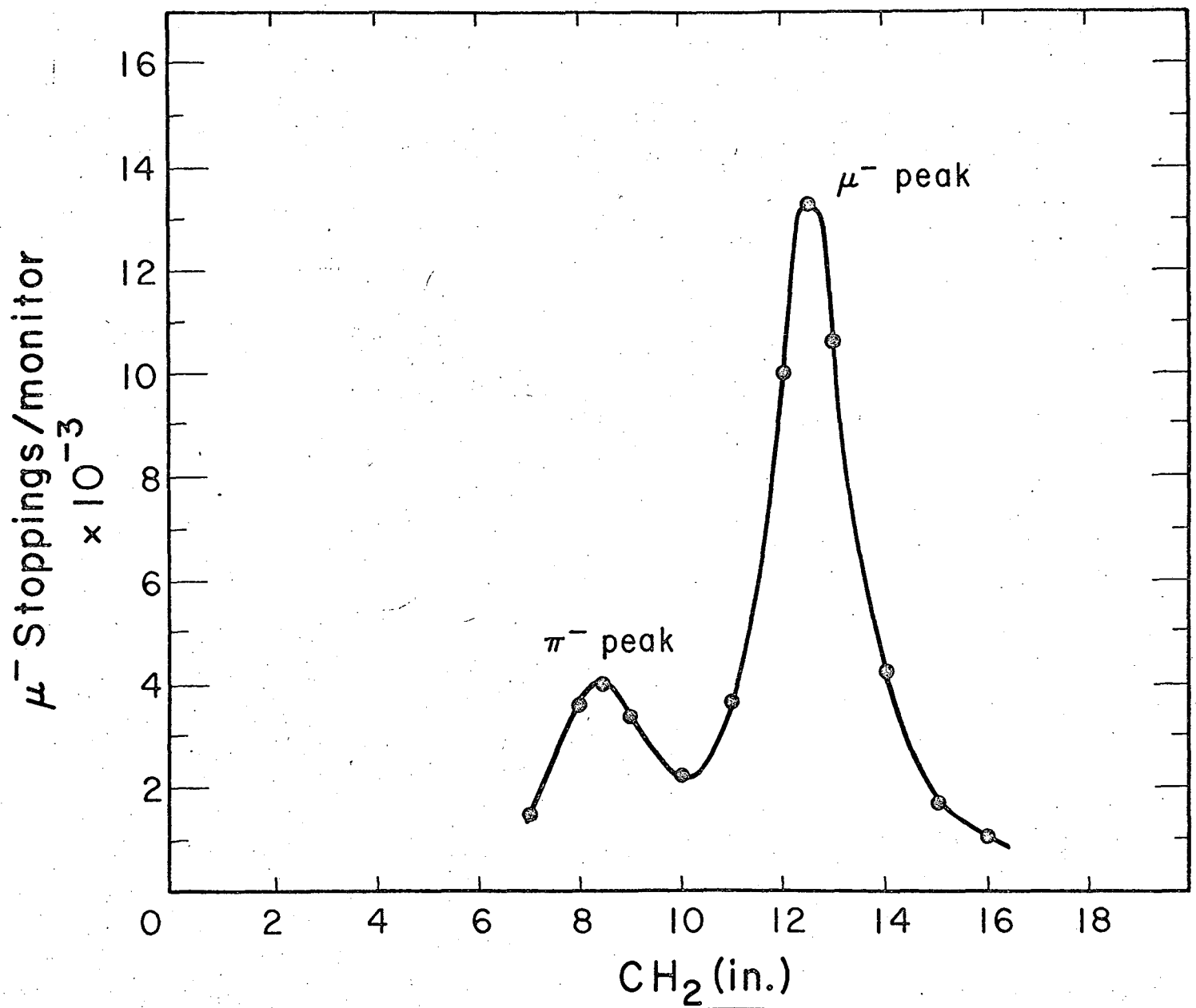


Fig. 2

MU-28054

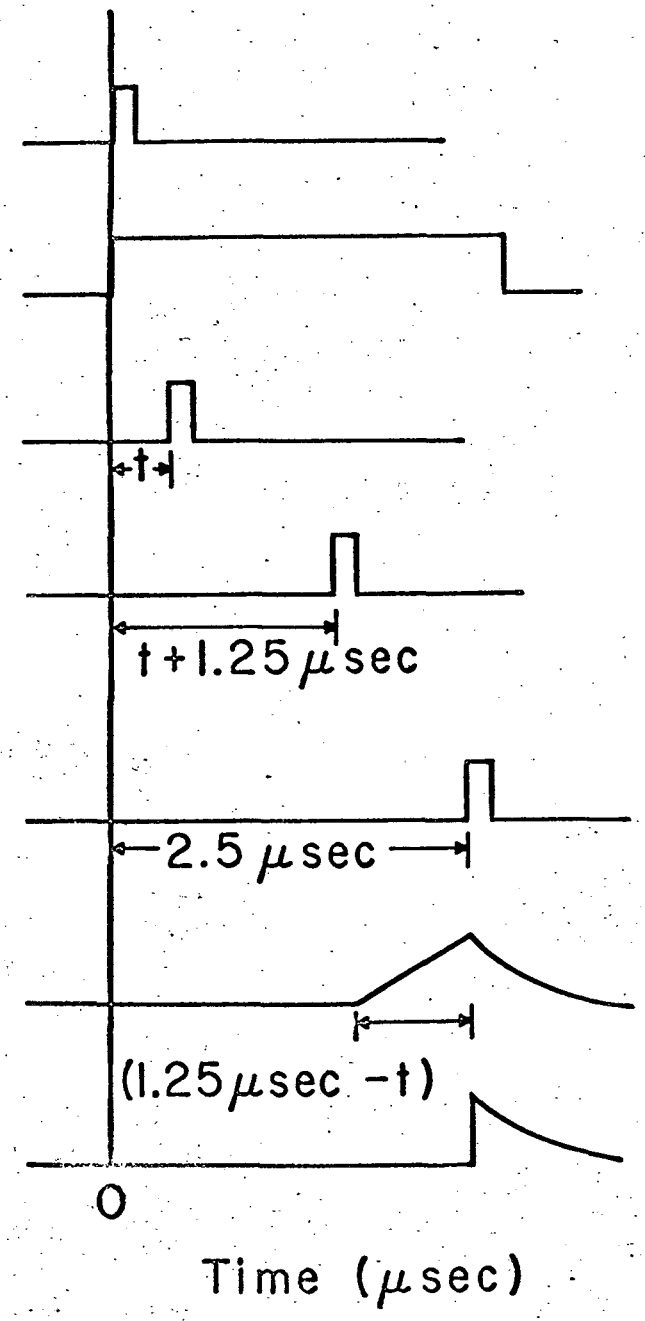


$\mu^-$ stop ($S_3 S_4 \overline{AC}$)

3-$\mu$sec gate generated by a $\mu^-$ stop

Neutron or gamma ($N\bar{A}$)

Delayed $N\bar{A}$ (start)

Delayed $S_3 S_4$ $\overline{AC}$ (stop)

T.H.C. output

Modified T.H.C. output

Fig. 3

MU-29349

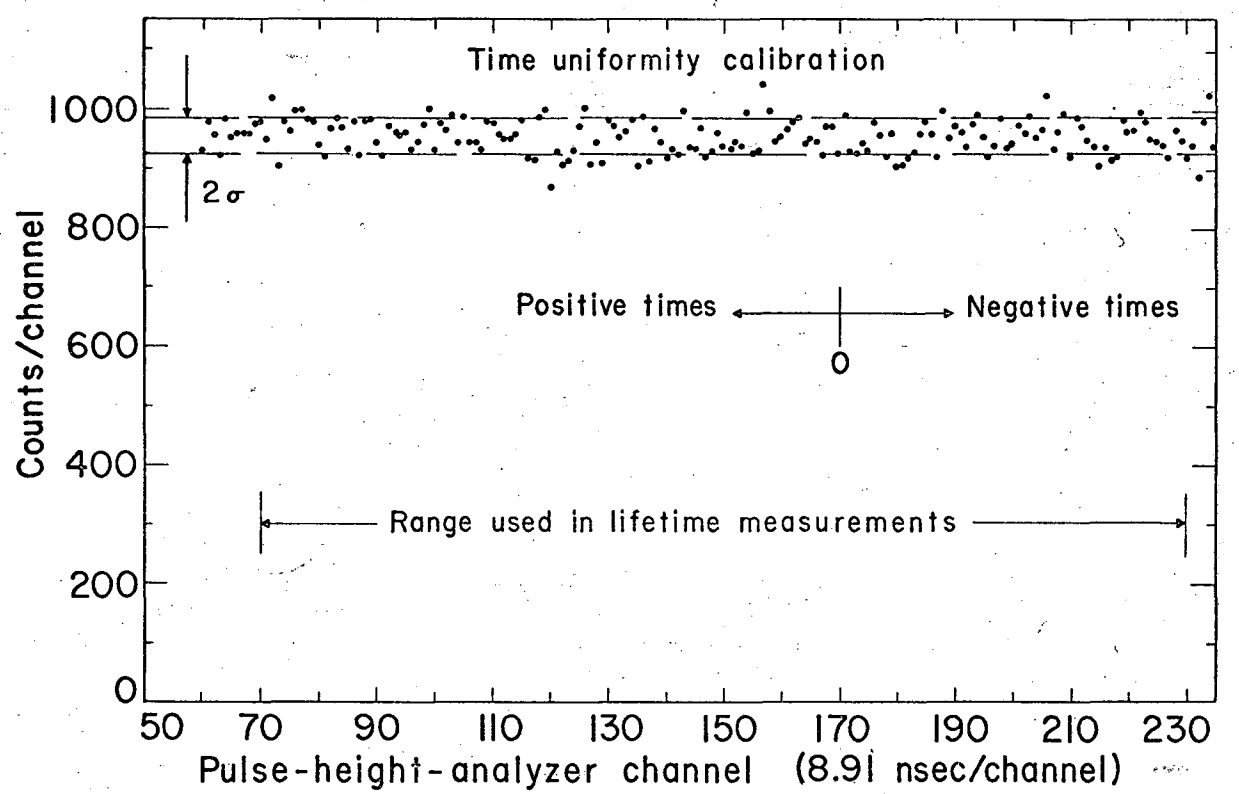
Time uniformity calibration
1000
800
600
400
200
0
Counts/channel
2σ
Positive times
Negative times
0
Range used in lifetime measurements
50
70
90
110
130
150
170
190
210
230
Pulse-height-analyzer channel (8.91 nsec/channel)
MUB-1252

Fig. 4

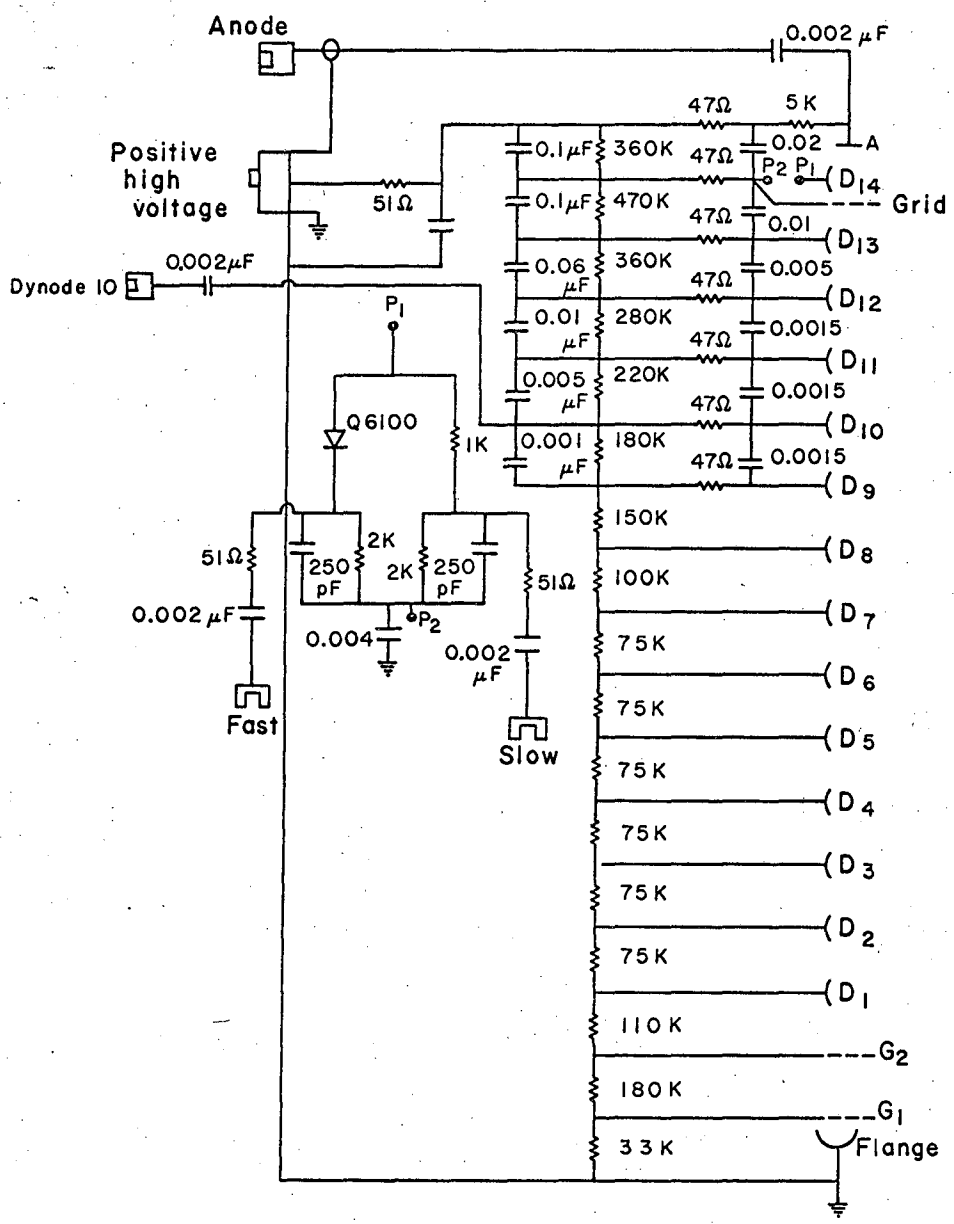
Anode
0.002 μF
47Ω
5 K
A
Positive high voltage
51Ω
0.1μF
360K
47Ω
0.02
P2 P1
D14
Grid
0.1μF
470K
47Ω
0.01
D13
0.002μF
Dynode 10
0.06 μF
360K
47Ω
0.005
D12
P1
0.01 μF
280K
47Ω
0.0015
D11
0.005 μF
220K
47Ω
0.0015
D10
Q6100
1K
0.001 μF
180K
47Ω
0.0015
D9
150K
D8
51Ω
250 pF
2K
2K
250 pF
51Ω
100K
D7
0.002 μF
P2
0.004
0.002 μF
75K
D6
Fast
Slow
75K
D5
75K
D4
75K
D3
75K
D2
75K
D1
110K
G2
180K
G1
33K
Flange
MUB-1330

Fig. 5

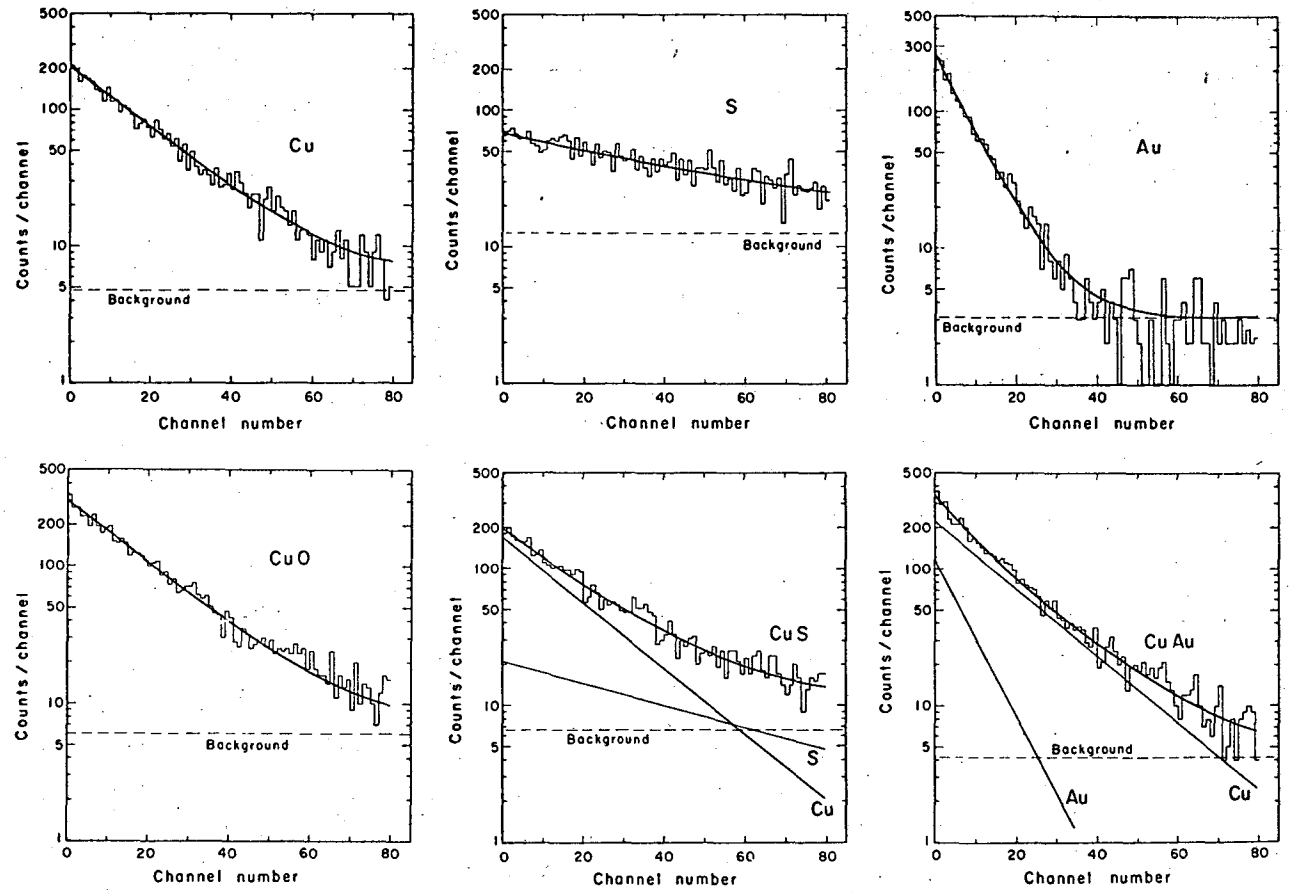
Cu
S
Au
CuO
CuS
Cu Au
Background
Counts / channel
Channel number
Au
Cu
S
MUB-1622

Fig. 6

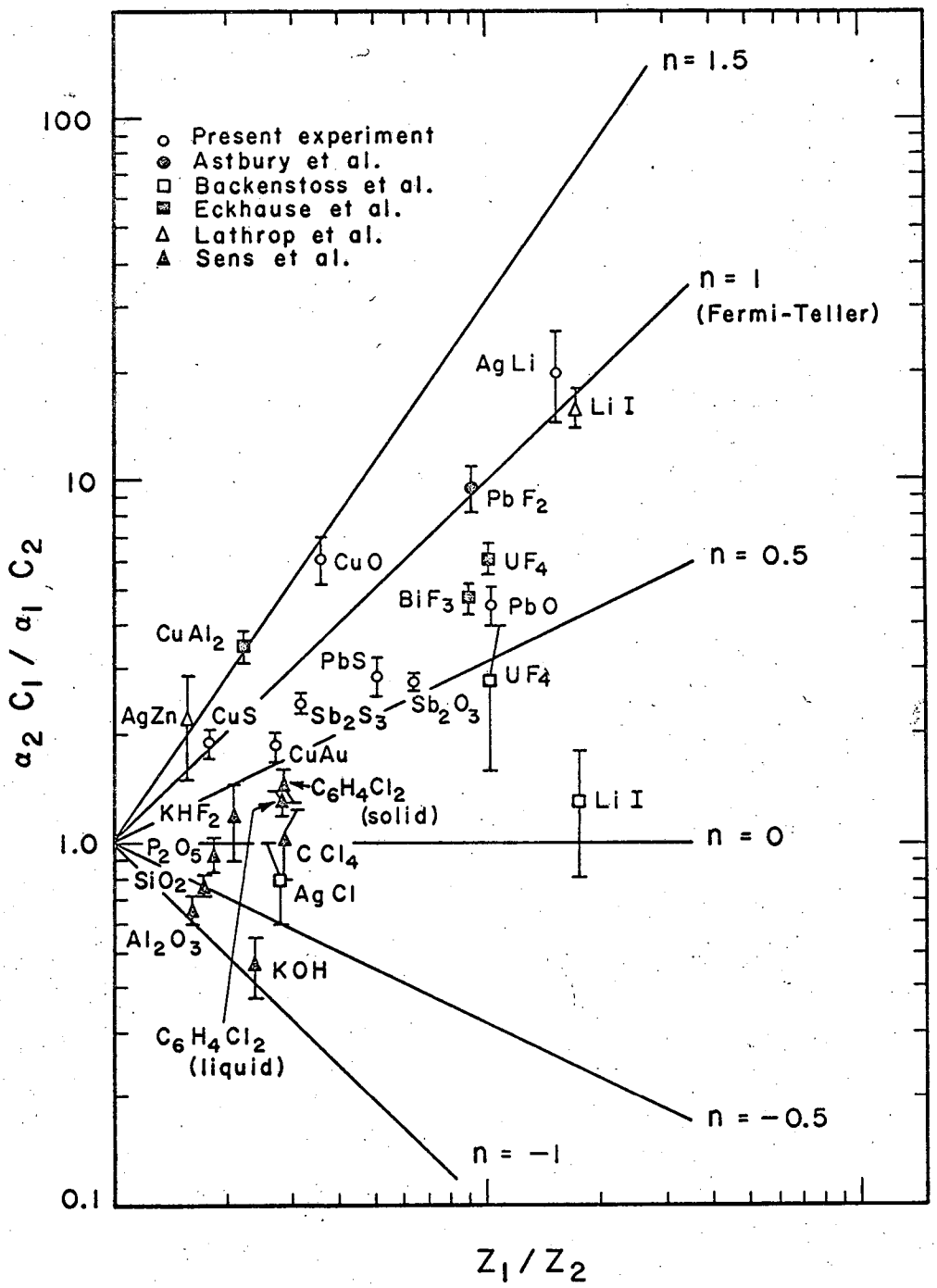


MUB-1333

Fig. 7

This report was prepared as an account of Government sponsored work. Neither the United States, nor the Commission, nor any person acting on behalf of the Commission:

A. Makes any warranty or representation, expressed or implied, with respect to the accuracy, completeness, or usefulness of the information contained in this report, or that the use of any information, apparatus, method, or process disclosed in this report may not infringe privately owned rights; or

B. Assumes any liabilities with respect to the use of, or for damages resulting from the use of any information, apparatus, method, or process disclosed in this report.

As used in the above, "person acting on behalf of the Commission" includes any employee or contractor of the Commission, or employee of such contractor, to the extent that such employee or contractor of the Commission, or employee of such contractor prepares, disseminates, or provides access to, any information pursuant to his employment or contract with the Commission, or his employment with such contractor.